Myosin light chain phosphorylation regulates barrier function by remodeling tight junction structure

Le Shen[1], Eric D. Black[1], Edwina D. Witkowski[1], Wayne I. Lencer[2], Vince Guerriero[3], Eveline E. Schneeberger[4] and Jerrold R. Turner[1,*]

[1]Department of Pathology, The University of Chicago, 5841 South Maryland Avenue, MC 1089,Chicago, IL 60637, USA
[2]GI Cell Biology, Combined Program in Pediatric Gastroenterology and Nutrition, and Departments of Pediatrics, Children's Hospital, Harvard Medical School, Boston, MA 02115, USA
[3]Departments of Animal Sciences and Molecular and Cellular Biology, University of Arizona, Tucson, AZ 85721, USA
[4]Department of Pathology, Massachusetts General Hospital, Harvard Medical School, Charlestown, MA 02129, USA
*Author for correspondence (e-mail: jturner@bsd.uchicago.edu)

Accepted 2 February 2006
Journal of Cell Science 119, 2095-2106 Published by The Company of Biologists 2006
doi:10.1242/jcs.02915

Summary

Epithelial tight junctions form a barrier against passive paracellular flux. This barrier is regulated by complex physiologic and pathophysiologic signals that acutely fine-tune tight junction permeability. Although actomyosin contraction and myosin light chain phosphorylation are clearly involved in some forms of tight junction regulation, the contributions of other signaling events and the role of myosin light chain phosphorylation in this response are poorly understood. Here we ask if activation of myosin light chain kinase alone is sufficient to induce downstream tight junction regulation. We use a confluent polarized intestinal epithelial cell model system in which constitutively active myosin light chain kinase, tMLCK, is expressed using an inducible promoter. tMLCK expression increases myosin light chain phosphorylation, reorganizes perijunctional F-actin, and increases tight junction permeability. TJ proteins ZO-1 and occludin are markedly redistributed, morphologically and biochemically, but effects on claudin-1 and claudin-2 are limited. tMLCK inhibition prevents changes in barrier function and tight junction organization induced by tMLCK expression, suggesting that these events both require myosin light chain phosphorylation. We conclude that myosin light chain phosphorylation alone is sufficient to induce tight junction regulation and provide new insights into the molecular mechanisms that mediate this regulation.

Supplementary material available online at
http://jcs.biologists.org/cgi/content/full/119/10/2095/DC1

Key words: Epithelial, Barrier, Claudin, Occludin, ZO-1

Introduction

Epithelia form barriers that define tissue compartments within higher organisms. Essential to the function of this barrier is the tight junction (TJ), which seals the paracellular space between individual epithelial cells against passive solute flux. We now know that at least one determinant of TJ ion selectivity is the specific pattern of claudin proteins expressed (Amasheh et al., 2002; Furuse et al., 1998a; Simon et al., 1999; Van Itallie et al., 2001). Modification of this pattern over extended intervals could explain disease-associated changes in TJ barrier function (Heller et al., 2005; Prasad et al., 2005). In the short term, TJ barrier function is acutely regulated by signal transduction cascades that do not depend on altered protein expression. In many cases these signaling cascades depend on the actin cytoskeleton, as they frequently require activation of rho proteins (Benais-Pont et al., 2003; Gopalakrishnan et al., 1998; Hirase et al., 2001; Jou et al., 1998; Nusrat et al., 1995; Walsh et al., 2001) or myosin light chain kinase (MLCK) (Berglund et al., 2001; Ma et al., 1999; Spitz et al., 1995; Turner et al., 1997; Wang et al., 2005; Zolotarevsky et al., 2002).

Myosin and actin form a dense ring that encircles the cell at the level of the adherens junction and TJ. Activation of actomyosin contraction, as assessed by phosphorylation of myosin II regulatory light chain (MLC), has been implicated in TJ regulation (Berglund et al., 2001; Ma et al., 1999; Spitz et al., 1995; Turner et al., 1997; Wang et al., 2005; Zolotarevsky et al., 2002). This frequently requires MLCK activity. For example, inhibition of MLCK can prevent or reverse TJ barrier losses induced by Na^+-nutrient co-transport (Turner et al., 1997), bacterial and parasitic infection (Dahan et al., 2003; Philpott et al., 1998; Scott et al., 2002; Yuhan et al., 1997; Zolotarevsky et al., 2002) and pro-inflammatory cytokines (Clayburgh et al., 2005; Ma et al., 2005; Wang et al., 2005; Zolotarevsky et al., 2002). Thus, it is now clear that MLCK-driven MLC phosphorylation is involved in signal transduction pathways that effect reduced barrier function in response to diverse stimuli (Turner, 2000).

Although studies using pharmacological MLCK inhibitors indicate a necessary role for MLCK, they are limited by the nonspecific effects inherent to most pharmacological agents. Moreover, inhibitor-based studies fail to consider the possibility that other signaling events known to be activated by upstream stimuli (Savkovic et al., 2003; Shiue et al., 2005; Sugi et al., 2001; Turner and Black, 2001; Zhao et al., 2004) may coordinate with myosin light chain phosphorylation to effect

barrier regulation. Thus, the question of whether myosin light chain phosphorylation alone is a sufficient signal to trigger acute barrier regulation remains unanswered.

Two previous studies have examined the role of myosin in epithelial TJ biogenesis and assembly (Gandhi et al., 1997; Hecht et al., 1996). These studies used epithelial cell lines stably transfected to express either a non-phosphorylatable MLC or a constitutively active truncated MLCK (tMLCK). This resulted in markedly reduced or increased MLC phosphorylation-dependent actomyosin contraction, respectively (Gandhi et al., 1997; Hecht et al., 1996). In both cases, epithelial cells lines with altered MLC phosphorylation were unable to develop significant barrier function, suggesting that TJ assembly was disrupted (Gandhi et al., 1997; Hecht et al., 1996). Unfortunately, structure of these incompletely developed TJs was not studied, probably reflecting the relatively limited understanding of TJ protein composition at the time. More importantly, these studies did not evaluate the response of assembled TJs to enhanced MLC phosphorylation, as only TJ assembly was studied. Thus, no available studies directly examine the effect of MLC phosphorylation on assembled TJs in mature epithelial monolayers: the physiologically relevant state.

The aim of these studies was to determine if MLCK-dependent MLC phosphorylation is sufficient to trigger TJ regulation in mature, assembled epithelial monolayers. Moreover, in the event that MLCK activation alone could trigger TJ regulation, we sought to determine morphological and biochemical changes in TJ structure that accompany MLC phosphorylation-induced barrier function decreases. We developed a Caco-2 cell line stably expressing an inducible transactivating element, Tet-off (Gossen and Bujard, 1992; Yu et al., 2001), that drives expression of a constitutively active truncated mutant of MLC kinase, tMLCK (Guerriero et al., 1986). By suppressing tMLCK expression until the Caco-2 cells formed fully differentiated polarized monolayers, we were able to test the role of MLCK in the acute regulation of TJ function.

Our data show that tMLCK-mediated MLC phosphorylation alone is sufficient to induce an increase in TJ permeability. This altered function is associated with structural redistribution of specific TJ proteins. Details of the MLC phosphorylation-induced functional, morphological and biophysical remodeling may explain the underlying mechanisms of the TJ regulation that occurs in response to physiologic and pathophysiologic stimuli.

Results

Inducible expression of tMLCK in epithelial monolayers

To develop a cell model for the inducible activation of MLCK, we first established an inducible expression ('Tet-off') system in Caco-2 cells (Yu et al., 2001). These cells were then stably transfected with an inducible construct to express a truncated myosin light chain kinase (tMLCK) lacking the calmodulin-binding inhibitory domain (Ito et al., 1991). The inducible expression approach used makes it possible for monolayers to differentiate and assemble TJs in the absence of transgene expression. Upon gene activation in mature, fully differentiated monolayers transgene protein activity and expression are detectable within 2 hours and continue to increase until

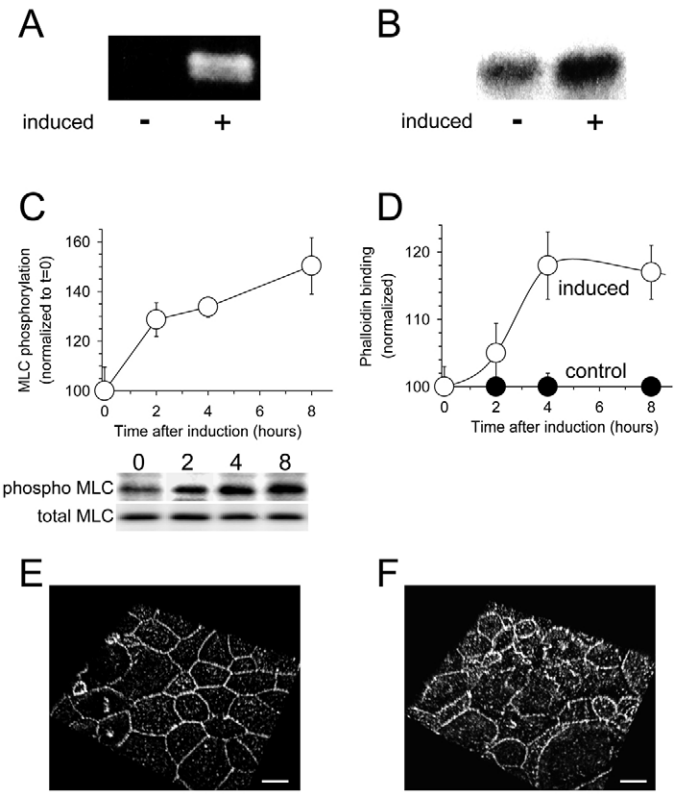

Fig. 1. Inducible tMLCK expression causes MLC phosphorylation and actin reorganization in differentiated Caco-2 monolayers. (A) tMLCK mRNA is readily detected by RT-PCR in Caco-2 cell monolayers after, but not before, induction. Digestion with *Nsi*I results in a doublet, verifying the identity of the PCR product. Results are representative of three or more experiments. (B) Increased tMLCK transcription is accompanied by a 4.7±0.4-fold increase in MLC kinase activity, assayed using an in vitro kinase assay. In the assay shown, which was performed with exogenous calmodulin and Ca^{2+}, the activity in lysates of cells without tMLCK expression represents endogenous MLC kinase. Results are representative of three or more independent experiments with this clone and at least two each with five independently generated clones. (C) Immunoblots using antisera specific for phosphorylated MLC show that induction of tMLCK expression causes progressive increases in endogenous MLC phosphorylation. Control immunoblots show that total MLC content did not change. Data from densitometric analysis of samples from the same experiment are shown in the graph. Data shown are means ± s.e.m. of triplicate samples and are representative of three or more independent experiments. Similar results were obtained with five independently generated clones. (D) tMLCK induction (open circles) caused increases in phalloidin binding that were not seen in uninduced (closed circles) monolayers. Total actin content, as assessed on western blots, was not changed. Data shown are means ± s.e.m. of quadruplicate samples and are representative of four independent experiments. (E) F-actin distribution was assessed by labeling with fluorescent phalloidin conjugates. The three-dimensional projection demonstrates typical perijunctional actin rings with focal mild intensifications within the ring and prominent apical microvillus cores. (F) Four hours after tMLCK induction, phalloidin-labeled F-actin shows perijunctional rings to be irregularly intensified, with brighter foci alternating with areas of reduced or unchanged labeling intensity. Bars, 10 μm.

Table 1. MLC phosphorylation-associated barrier regulation in intestinal epithelia

	Increased MLC phosphorylation	Reduced resistance	Size selectivity	Reference
tMLCK expression (cultured monolayers)	150%	18%	mannitol >> inulin	
Na^+-nutrient cotransport (cultured monolayers)	208%	22%	mannitol >> inulin	Turner et al., 1997
Na^+-nutrient cotransport (isolated mucosae)	145%	22%	mannitol >> inulin	Berglund et al., 2001; Fihn et al., 2000

reaching a steady-state plateau after 8-16 hours. RT-PCR analysis of tMLCK expression shows that tMLCK mRNA is not detectable in the absence of induction, indicating successful repression of tMLCK transcription. Induction readily induces tMLCK mRNA transcription (Fig. 1A) and increases cellular MLC kinase activity 4.7±0.4-fold (Fig. 1B). As expected for tMLCK, the increase in MLC kinase activity did not depend on the presence of divalent cations. Thus, this Caco-2 cell model allows inducible tMLCK mRNA transcription and MLC kinase activation in mature, fully differentiated monolayers.

tMLCK expression increases MLC phosphorylation and modifies actin organization

Although tMLCK expression is clearly regulated by this inducible expression system, it is crucial to determine if the increase in MLC kinase activity detected in cell lysates (Fig. 1B) reflects increases in intracellular MLC phosphorylation. For example, it is possible that compensatory increases in MLC phosphatase or other counter-regulatory activities occur. Thus, we assessed MLC phosphorylation by induction of tMLCK expression in fully differentiated Caco-2 monolayers with completely assembled TJs. tMLCK expression resulted in increased intracellular MLC phosphorylation, with maximal MLC phosphorylation equal to 150±11% of levels in the control achieved within 8 hours of induction (Fig. 1C). This increase is comparable in magnitude to the MLC phosphorylation that occurs in response to physiological stimuli in cultured intestinal epithelial monolayers and isolated mucosae (Table 1) (Berglund et al., 2001; Turner et al., 1997). Similar results were obtained with at least five independently generated clones. This Caco-2-inducible tMLCK model is therefore suitable for studies of the effects of MLCK activation in fully differentiated intestinal epithelial monolayers.

Many studies have linked MLC phosphorylation to increased actin polymerization and stress fiber assembly (Goeckeler and Wysolmerski, 1995; Katoh et al., 2001). Since both actin and myosin are intimately associated with the TJ, we therefore asked if actin assembly was altered by tMLCK expression. F-actin content was assessed by quantitative analysis of phalloidin binding (Howard and Oresajo, 1985a; Howard and Oresajo, 1985b; Shen and Turner, 2005). Within 4 hours of tMLCK induction, phalloidin binding increased by 18±1% (Fig. 1D), consistent with increased microfilament number or length. This was not due to increased actin synthesis, because SDS-PAGE immunoblot analyses showed no change in total actin content. Inhibition of MLCK activity completely prevented increases in phalloidin binding, suggesting that the enzymatic activity of tMLCK was responsible for the observed changes. Morphological assessment of F-actin labeled with fluorescent phalloidin conjugates showed typical perijunctional actin rings in control monolayers (Fig. 1E). Within 4 hours of tMLCK induction, phalloidin labeling of perijunctional actin rings was irregularly intensified, with brighter foci alternating with areas of reduced or unchanged labeling intensity (Fig. 1F).

TJ permeability increases after tMLCK expression

The data above show that induction of tMLCK expression in mature, fully differentiated Caco-2 monolayers with assembled TJs results in MLC phosphorylation and reorganization of perijunctional F-actin. To evaluate the effect of tMLCK expression on TJ barrier function we measured transepithelial electrical resistance (TER) before and after tMLCK induction. Progressive decreases in TER occurred during induction of tMLCK expression, with TER loss apparent within 2 hours. TER fell by 18±2% at 8 hours after doxycycline washout (Fig. 2A). This was maximal, as the TER reductions regularly observed after 24-48 hours of induction ranged from 17% to 26% in individual experiments using the clone shown and five other independently generated clones. The magnitude of this TER loss was remarkably similar to that observed after initiation of Na^+-nutrient co-transport in cultured monolayers and isolated mucosae (Table 1) (Atisook et al., 1990; Berglund et al., 2001; Turner et al., 1997). Moreover, these TER reductions occurred with similar kinetics to increases in MLC phosphorylation (r=0.94). To determine if the observed effects on TER required increased MLC kinase activity, kinase activity was inhibited in monolayers expressing tMLCK. Preliminary experiments verified that this treatment was sufficient to normalize MLC phosphorylation levels in monolayers expressing tMLCK. This MLCK inhibition, of both tMLCK and endogenous MLCK (Clayburgh et al., 2004; Ikebe et al., 1987; Ito et al., 1991), rescued the TER drop recorded in monolayers expressing tMLCK (Fig. 2B). Thus, the regulation of TJ barrier function that occurs following induction of tMLCK expression requires MLCK activity.

Recent studies have shown dissociation between TER and TJ permeability to macromolecular tracers following transgenic expression of selected TJ proteins (Balda et al., 1996; McCarthy et al., 1996; Van Itallie et al., 2001). By contrast, in vivo and in vitro physiological TER regulation associated with MLC phosphorylation causes size-selective increases in TJ permeability (Fihn et al., 2000; Turner et al., 1997). We therefore asked if, like physiological MLCK-dependent TJ regulation, tMLCK expression causes size-selective increases in TJ permeability. As probes we used radiolabeled mannitol and inulin, which have hydrodynamic radii of 3.6 Å and 11.5 Å, respectively. Previous studies have shown that physiological MLCK-dependent TJ regulation increases permeability to mannitol, but not inulin, in cultured monolayers and isolated mucosae (Fihn et al., 2000; Turner et al., 1997). Induction of tMLCK expression in Caco-2 cell monolayers caused a 40±4% increase in transepithelial flux of mannitol (Fig. 2C). By contrast, the transepithelial flux of inulin was not changed by tMLCK expression (Fig. 2C). Thus,

tMLCK-mediated MLC phosphorylation effects size-selective increases in TJ permeability that recapitulate physiological TJ regulation in vitro and in vivo (Table 1) (Fihn et al., 2000; Turner et al., 1997).

tMLCK expression induces reorganization of TJ membrane microdomains

TJ membranes have biochemical characteristics of lipid microdomains that are operationally defined as detergent-insoluble, low-density, glycolipid- and cholesterol-rich membranes (Nusrat et al., 2000). These detergent-insoluble membranes are enriched in TJ proteins (Nusrat et al., 2000) and the TJ proteins within these fractions are thought to represent those specifically associated with the TJ (Nusrat et al., 2000). For example, more than 90% of hyperphosphorylated occludin, which is thought to represent the tight junction-associated pool, is present in these detergent-insoluble fractions (Nusrat et al., 2000). This represents between 5% and 15% of total cellular occludin (Bruewer et al., 2003; Clayburgh et al., 2005; Nusrat et al., 2000; Nusrat et al., 2001; Wang et al., 2005). Disruption of these cholesterol-rich membrane domains by extraction of plasma membrane cholesterol disrupts TJ barrier properties (Francis et al., 1999) and TJ proteins are lost from detergent-insoluble membrane fractions when TJ barrier function is disrupted by pathophysiological stimuli (Bruewer et al., 2003; Clayburgh et al., 2005; Nusrat et al., 2001; Wang et al., 2005). We therefore evaluated the effect of tMLCK expression on targeting of TJ proteins to detergent-insoluble membrane fractions. We initially asked if MLC phosphorylation might alter the proportion of these proteins in the detergent-insoluble fractions. Neither the proportion of total occludin, claudin-1 or claudin-2 present in these fractions, as opposed to detergent-soluble membranes, nor total cellular content of these proteins was affected by tMLCK expression. However, tMLCK expression resulted in a shift of occludin to higher-density fractions within the detergent-insoluble pool. The peak fractions of occludin shifted from a density of 1.081 g/ml to 1.090 g/ml after induction of tMLCK expression (Fig. 3). This shift corresponded to a marked shift in the overall distribution of occludin within the detergent-insoluble membranes. Although the peak fraction of claudin-1 was also shifted by tMLCK expression, the overall distribution of claudin-1 within the gradient did not change significantly (Fig. 3). The density of claudin-2-containing membranes was also unchanged after tMLCK expression. Despite the unchanged density of claudin-containing detergent-insoluble membranes after tMLCK expression, we considered the possibility that the density of a large subset of low-density, glycolipid- and cholesterol-rich membranes was changed by tMLCK expression. To evaluate this we used a general marker of low-density glycolipid-rich membranes, ganglioside GM1 (Wolf et al., 1998). Like claudin-1, and claudin-2, ganglioside GM1 was present in the detergent-insoluble low-density membrane fractions and the density of the GM1-containing fractions was not changed by tMLCK expression (Fig. 3). Thus, a global increase in the density of detergent-insoluble low-density membranes did occur after induction of tMLCK expression. This indicates that the observed shift in the density at which occludin separates represents a specific effect on occludin-containing detergent-insoluble membranes.

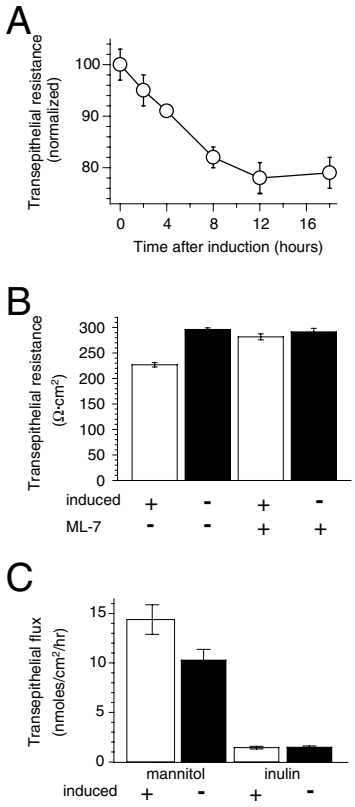

Fig. 2. tMLCK induction reduces barrier function. (A) TER decreases progressively after tMLCK induction. TER, normalized to control monolayers handled in parallel, fell progressively after doxycycline washout. TER 8-18 hours after tMLCK induction was similar to that seen as much as 48 hours after doxycycline washout (data not shown). Data shown are means ± s.e.m. of triplicate samples and are representative of more than ten independent experiments. Similar results were obtained with five independently generated clones. (B) Inhibition of myosin light chain kinase by addition of 10 μM ML-7 to control monolayers (closed bars) and monolayers expressing tMLCK (open bars) causes TER of the latter to increase to that of control monolayers not expressing tMLCK. tMLCK expression was induced for 18 hours and ML-7 added for 1 hour before TER measurement. Data shown are means ± s.e.m. of triplicate samples and are representative of four independent experiments. (C) tMLCK expression increases transepithelial flux of the small paracellular tracer mannitol, but not inulin, demonstrating size-selective increases in paracellular permeability as a consequence of tMLCK-induced MLC phosphorylation. Data shown are means ± s.e.m. of triplicate samples and are representative of three independent experiments.

TJ ultrastructure is not significantly changed by tMLCK expression

Previous studies have reported the presence of dilatations within the TJ in response to activation of Na^+-glucose co-transport in isolated intestinal mucosae (Atisook et al., 1990; Atisook and Madara, 1991; Madara and Pappenheimer, 1987). Although recognizable by transmission electron microscopy, these were especially impressive when examined by freeze-fracture electron microscopy (Madara and Pappenheimer, 1987). The latter revealed that the dilatations consisted of expansions of intrajunctional compartments bounded by TJ

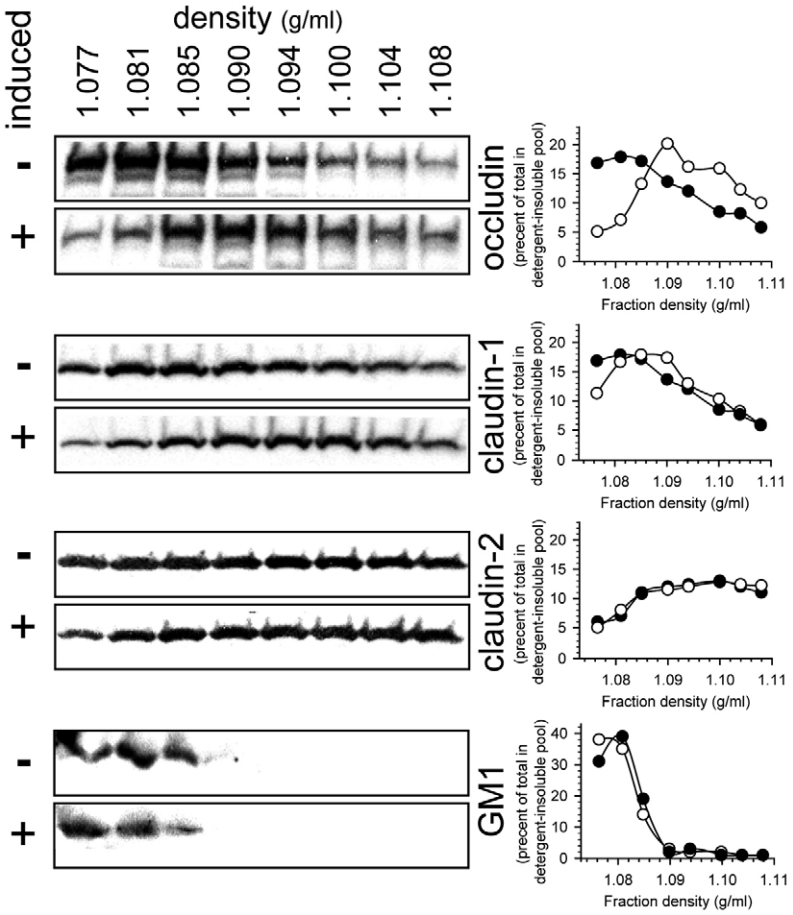

Fig. 3. TJ membranes are modified by tMLCK expression. Detergent-insoluble low-density membranes were isolated from control monolayers without tMLCK induction (closed circles on graphs) or 8 hours after induction of tMLCK expression (open circles on graphs). Fractions were analyzed by SDS-PAGE immunoblot for occludin, claudin-1, and claudin-2. GM1 ganglioside was detected with peroxidase-conjugated cholera toxin B subunit. Densitometric analysis (right) shows that tMLCK expression causes occludin to shift to fractions of higher density, whereas claudin-1, claudin-2 and GM1 distributions were not significantly changed. Results are typical of six independent experiments.

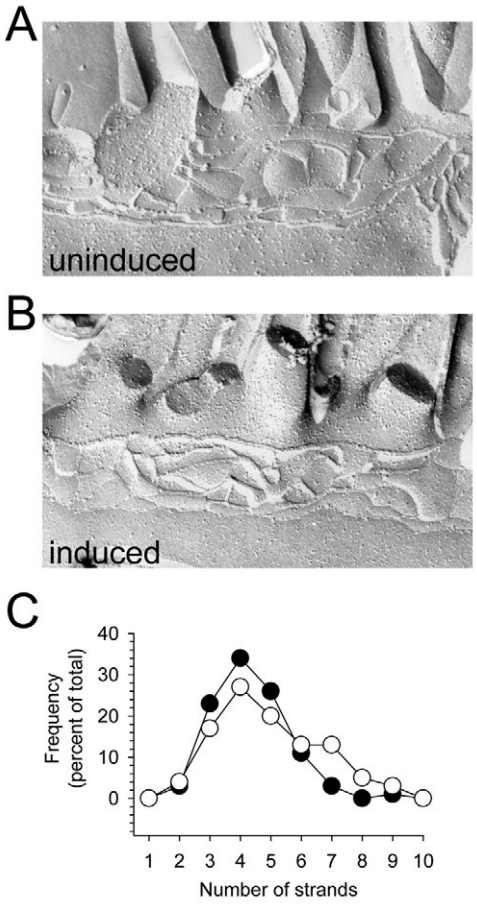

Fig. 4. TJ ultrastructure and strand number are not altered by tMLCK expression. (A,B) Representative images of TJ from monolayers not induced (A) or induced (B) to express tMLCK. Magnification, 62,500×. (C) The number of strands in each TJ replica was counted at 160 nm intervals over a total distance of 195 μm and 185 μm in monolayers induced (open circles) or not induced (closed circles) to express tMLCK, respectively. This resulted in 56 and 54 strand counts in induced and uninduced monolayers, respectively. The histogram shows the frequency with which each strand number was observed. There was no significant difference between induced and uninduced monolayers.

strands (Madara and Pappenheimer, 1987). To determine whether these changes were associated with MLC phosphorylation in the absence of stimulated Na^+-glucose co-transport, TJ ultrastructure was examined in freeze-fracture replicas of monolayers with or without tMLCK expression (Fig. 4A,B). Multiple replicas were examined and no significant difference was detected in the morphology or organization of the TJ strands. Most notably, intrajunctional dilatations were not detected. Morphometric analysis of strand number revealed no detectable differences induced by tMLCK expression. TJs in monolayers with or without tMLCK expression were predominantly composed of four strands, with a range of two to nine strands (Fig. 4C). Further morphometry showed that TJ height was 0.195±0.078 μm in the absence of tMLCK expression (181 profiles with a total length of 35.3 μm examined) and increased marginally, to 0.208±0.066 μm height (194 profiles with a total length of 40.3 μm examined), in monolayers expressing tMLCK (P=0.043). Although statistically significant, we interpret these changes as small and of minimal biological significance. These data therefore show that the ultrastructural TJ reorganization, primarily intrajunctional dilatations, previously observed following activation of Na^+-glucose cotransport in isolated intestinal mucosae cannot be reproduced by MLC phosphorylation alone.

ZO-1 distribution is modified by tMLCK expression and activity

Redistribution of specific TJ proteins during MLC phosphorylation-dependent TJ regulation has not been described in detail. One ultrastructural study reported ZO-1 dissociation from TJ fibrils following activation of Na^+-glucose co-transport in isolated intestinal mucosae (Madara et al.,

1993). More complex stimuli associated with MLC phosphorylation, including bacterial infection and cytokine treatment, have been associated with in vitro and in vivo TJ protein reorganization (Clayburgh et al., 2005; Hopkins et al., 2003; Ivanov et al., 2004a; Ivanov et al., 2004b; Ma et al., 2005; Shifflett et al., 2005; Simonovic et al., 2000; Tomson et al., 2004; Wang et al., 2005). However, it is clear that these stimuli activate many signaling pathways in addition to MLC kinase (Bruewer et al., 2003; Bruewer et al., 2005; Edens et al., 2002; Hopkins et al., 2003; Ivanov et al., 2004a; Ma et al., 2004; Tomson et al., 2004). We therefore asked whether specific alterations in TJ protein distribution could be induced by tMLCK-mediated MLC phosphorylation. When viewed en face, in the *x-y* plane, ZO-1 profiles in control monolayers are generally smooth arc-like structures (Fig. 5A). Occasional gentle undulations impart a focal waviness to the profiles. Within 4 hours of tMLCK induction this appearance was markedly modified; smooth arc-like ZO-1 profiles were difficult to appreciate. Almost all areas showed the gentle undulations that were focally present in control monolayers (Fig. 5B). Moreover, in many areas, ZO-1 profiles were dramatically rearranged into an irregular series of fine and course undulations (Fig. 5B). Similar ZO-1 reorganization occurred in five independently generated clones with inducible tMLCK expression.

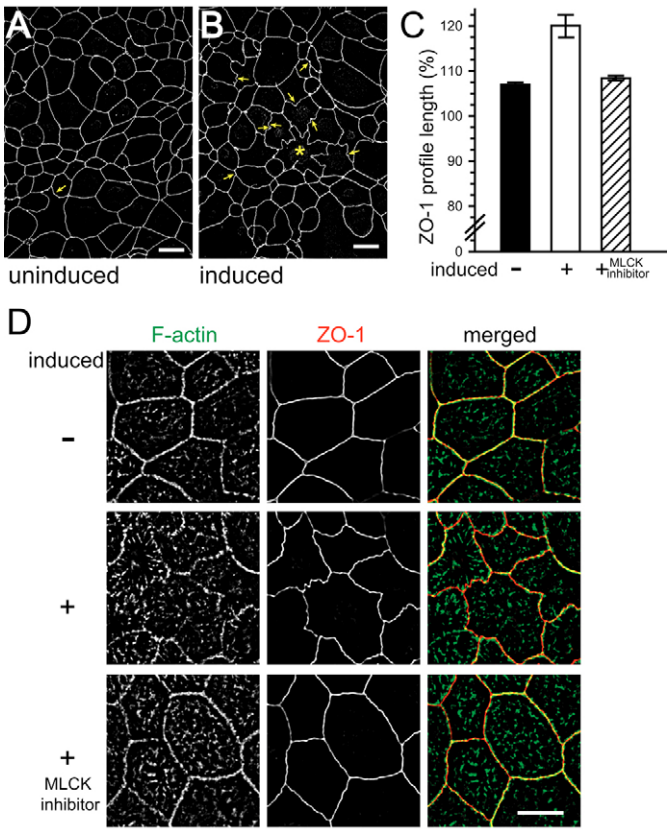

Fig. 5. Distributions of ZO-1 and perijunctional F-actin are altered by tMLCK expression. (A) ZO-1 profiles in monolayers not expressing tMLCK are smooth and arc-like. Only occasional mild undulations are present (arrow). (B) tMLCK expression causes ZO-1 profiles to be reorganized into irregularly undulating patterns (image shown is 4 hours after induction). These undulations are present throughout the monolayer (arrows). In addition, occasional cells are extremely affected (asterisk). Although relatively uncommon in induced cultures, such cells were never seen in monolayers without tMLCK expression. (C) Quantitative analysis of ZO-1 profile length shows that it is increased significantly (n=40 per condition; P<0.001) by tMLCK expression. MLCK inhibition using 250 μM PIK (Zolotarevsky et al., 2002) decreased profile length to levels observed in cells not expressing tMLCK (n=40 per condition; P>0.1). (D) Smooth F-actin and ZO-1 profiles are reorganized into irregular undulations 8 hours after tMLCK induction. Addition of 250 μM PIK (Zolotarevsky et al., 2002) during this tMLCK induction prevented the formation of undulations in both F-actin and ZO-1 distributions. Representative images are shown. Bars, 10 μm.

Subjective semi-quantitative analyses showed that the number of TJ segments, i.e. the interval between two adjacent tricellular zones, with ZO-1 undulations of any sort increased from 16±4% before to 55±3% after tMLCK expression (n=878; P<0.001). To characterize these changes in a completely quantitative fashion the actual ZO-1 profile length between adjacent tricellular zones was measured. To correct for normal segment length variation, linear distance between adjacent tricellular zones was used to normalize ZO-1 profile length for each segment measured. The ZO-1 profile length was increased from 107±0.5% to 120±2.4% of linear length by tMLCK expression (n=40 per condition; P<0.001) (Fig. 5C).

To better define the reorganization of perijunctional F-actin and ZO-1 proteins that was induced by tMLCK expression, we analyzed double-labeled preparations at higher magnification. Perijunctional F-actin was distorted into undulating profiles by tMLCK expression (Fig. 5D). However, this was less prominent than the changes in ZO-1 and quantitative analysis of F-actin profile length did not show a significant difference after tMLCK expression (Fig. 7). This quantitative difference and the merged images, which show a greater proportion of the ZO-1 profile without prominent F-actin colocalization after tMLCK expression, suggest the presence of focal separations of F-actin from ZO-1 (Fig. 5D, also see Fig. 8 for a very high magnification view).

The morphological changes described above correlate with the decreased TER induced by tMLCK expression. In the case of decreased TER, the effects of tMLCK expression could be completely prevented by inhibition of kinase activity (Fig. 2B). We therefore asked whether kinase inhibition can prevent the ZO-1 undulations that were induced by tMLCK expression. Examination of monolayers expressing tMLCK after kinase inhibition showed that this treatment blocked redistribution of ZO-1 into the undulating profiles seen in monolayers expressing tMLCK (Fig. 5D). Quantitative analysis confirmed that the increase in ZO-1 profile length induced by tMLCK expression was completely blocked; ZO-1 profile length in tMLCK-expressing monolayers was reduced from 120±2.4% to 108±0.5% of linear length by MLCK inhibition (n=40 per condition; P<0.001) (Fig. 5D). This length after MLCK inhibition (108%) is no different to the ZO-1 profile length of 107% measured in control monolayers not expressing tMLCK (n=40 per condition; P>0.1). Thus, the ZO-1 redistribution induced by tMLCK expression requires kinase activity.

Occludin, but not claudin-1 and claudin-2, is redistributed with ZO-1 after tMLCK expression

To define whether the ZO-1 redistribution induced by tMLCK expression represented a wholesale TJ reorganization, we also

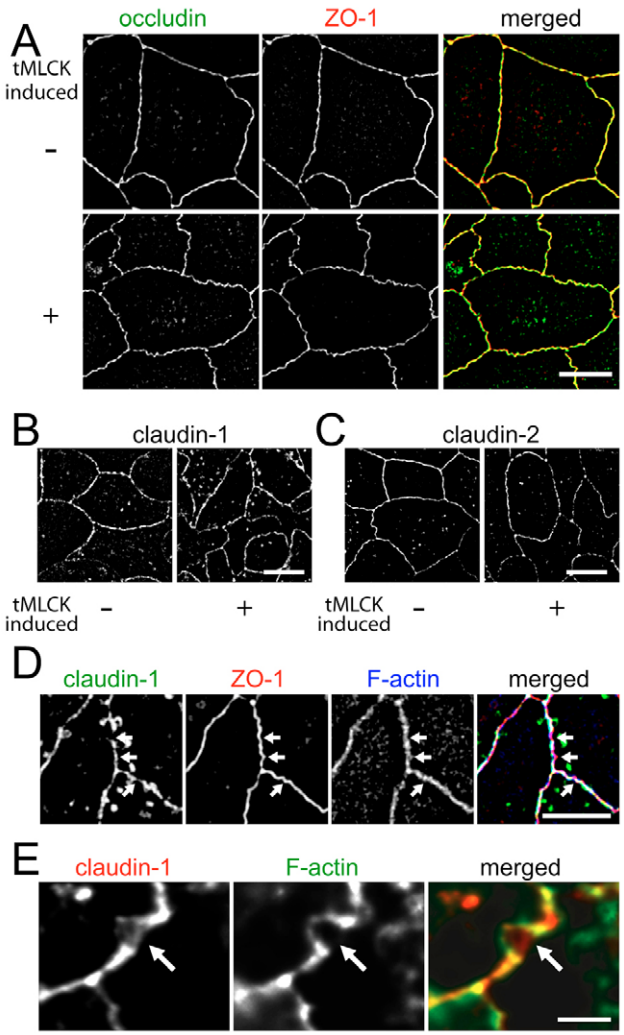

Fig. 6. Distribution of occludin, but not claudin-1 and claudin-2, is altered by tMLCK expression. (A) Like ZO-1, arc-like occludin profiles are also remodeled to include irregular undulations 4 hours after induction of tMLCK expression. Although redistributed, occludin remains colocalized with ZO-1 (see merged images). Representative images are shown. (B) Rare claudin-1 undulations can be found before and 4 hours after induction of tMLCK expression. However, overall, tMLCK expression did not cause significant changes in claudin-1 localization. This is confirmed by quantitative analysis (Fig. 7). Representative images are shown. (C) Like claudin-1, focal claudin-2 undulations can be found before and 4 hours after induction of tMLCK expression. Also like claudin-1, the overall distribution of claudin-2 was not changed after induction of tMLCK expression. This is confirmed by quantitative analysis (Fig. 7). Representative images are shown. (D) Triple-label image of claudin-1 (green), ZO-1 (red) and F-actin (blue) in cells expressing tMLCK. Although undulations of the ZO-1 profile can be easily seen (arrows), no such undulations are apparent in the claudin-1 image. F-actin shows some minimal undulations, but to a far lesser degree than ZO-1. The absence of claudin-1 at sites of undulations can also be appreciated in the merged image. (E) High-magnification analysis of undulations in monolayers expressing tMLCK shows that, at these sites, F-actin (green) staining intensity is reduced (arrows). Claudin continues directly across the site of F-actin undulation, without deviating from the arc of the junction. However, claudin-1 labeling is decreased at this site (also seen in panel D). Bars, 10 μm (A-C); 5 μm (D); 2.5 μm (E).

evaluated the distributions of occludin, claudin-1, and claudin-2 before and after tMLCK expression. Like ZO-1, occludin distribution in the *x-y* plane was reorganized from smooth arcs into a series of fine undulations (Fig. 6A). Quantitative analysis of occludin profile length showed that this was increased, from 106±0.6% to 116±2.0% of linear length by tMLCK expression ($P<0.001$) (Fig. 7). These data suggest that the reorganization of occludin and ZO-1 may be linked. To assess this we directly compared ZO-1 and occludin distributions after tMLCK expression (Fig. 6A). These proteins remained colocalized, even at the sites of undulations (see Fig. 8 for a very high magnification view). Therefore, despite marked redistribution, ZO-1 and occludin maintain their spatial association after tMLCK expression.

We also assessed the effects of tMLCK expression on the claudin distribution by examining the two principal claudin isoforms expressed in these monolayers: claudin-1 and claudin-2. To avoid confusion with the large lateral membrane pools of claudin-1 in Caco-2 cell monolayers, the TJ was defined as the *z* plane with maximal ZO-1 staining. Claudin-1 was only minimally redistributed by tMLCK expression (Fig. 6B). High-magnification images comparing the distribution of claudin-1 to ZO-1 and F-actin in tMLCK-expressing monolayers confirms that, at sites of ZO-1 undulation, claudin-1 distribution is generally unaffected (Fig. 6D) or, in some cases, shows a focal reduction in staining intensity (Fig. 6E). Quantitative analysis confirmed that, unlike ZO-1 and occludin, claudin-1 profile length was unchanged after tMLCK expression; claudin-1 profile lengths before and after tMLCK expression were 106±2.0% and 110±0.9%, respectively (Fig. 7). Although only small amounts of claudin-2 were present at the lateral membranes of Caco-2 monolayers, the TJ was defined as the *z* plane with maximal ZO-1 staining to avoid misinterpretation owing to extra-TJ claudin-2. Like claudin-1, claudin-2 distribution was also unaffected by tMLCK expression (Fig. 6C). Claudin-2 profile lengths before and

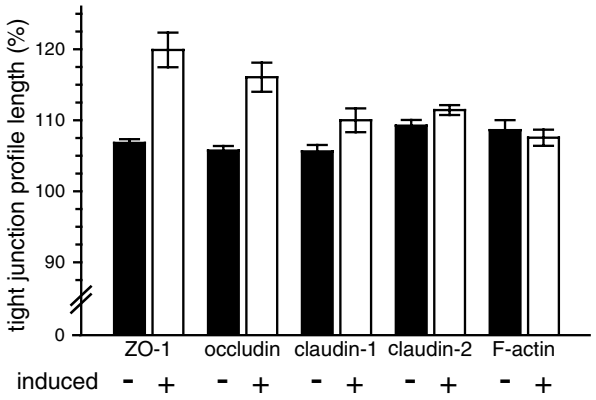

Fig. 7. Quantitative analysis of tight junction protein profile length. Profile length was assessed in monolayers stained for the indicated TJ protein using well-oriented en face images at the plane of the TJ. Actual profile length was normalized to linear length (mean ± s.e.m.), as described in the Materials and Methods. tMLCK expression caused marked increases in ZO-1 and occludin profile length, consistent with the presence of many undulations. By contrast, claudin-1, claudin-2 and F-actin profile length were unchanged by tMLCK expression.

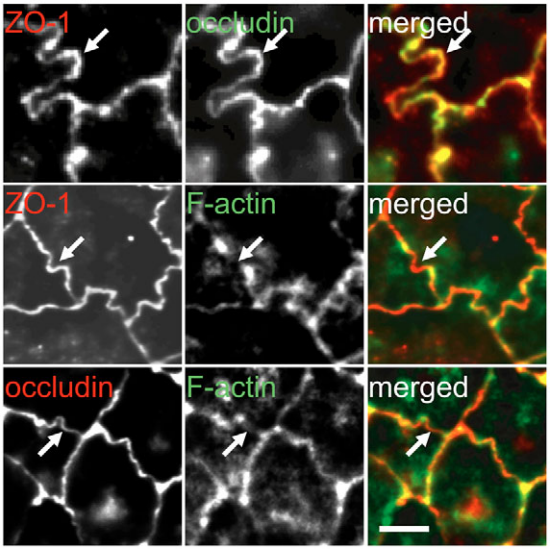

Fig. 8. Perijunctional actin and TJ proteins are focally separated by tMLCK expression. High-magnification analysis of undulations in monolayers expressing tMLCK shows that, at these sites, F-actin staining intensity is reduced (arrows). In cells labeled for either ZO-1 or occludin and F-actin this results in the undulated region staining red (ZO-1 or occludin) in the merged image, rather than yellow, owing to loss of F-actin staining (green) at these sites (arrows). By contrast, analysis of cells double labeled for ZO-1 and occludin shows that these two proteins remain precisely colocalized at sites of undulations. Bar, 2.5 μm.

after tMLCK expression were 109±0.8% and 111±0.7%, respectively (Fig. 7). Thus, unlike ZO-1 and occludin, claudin-1 and claudin-2 distributions were not significantly modified by tMLCK expression.

tMLCK expression causes focal separation of ZO-1 and occludin from perijunctional actin

The qualitative and quantitative data suggest that ZO-1 and occludin are reorganized into irregular undulating profiles by tMLCK expression. F-actin is clearly reorganized qualitatively, but in a manner different to that of ZO-1 and occludin. This too is supported by the quantitative analyses and suggests that focal morphological separation of ZO-1 and occludin from F-actin may be induced by tMLCK expression. To investigate this possibility, the distributions of these proteins were examined at high magnification in double-labeled preparations. Even at sites of extreme undulations, ZO-1 and occludin remained precisely colocalized (Fig. 8). By contrast, F-actin was frequently separated from ZO-1 and occludin at sites of undulations, such that in some focal planes it appeared that F-actin was absent from all or part of the irregular ZO-1 or occludin profiles (Fig. 8).

Discussion

Inhibitor studies have indicated that MLCK activation, as assessed by MLC phosphorylation, is necessary for TJ regulation secondary to diverse physiological and pathophysiological stimuli (Hopkins et al., 2003; Scott et al., 2002; Turner et al., 2000; Turner et al., 1997; Yuhan et al., 1997; Zolotarevsky et al., 2002). However, the nonspecific nature of pharmacologic agents, the complexity of the stimuli used, and the absence of appropriate experimental models has made it impossible to determine if MLC phosphorylation alone is sufficient to trigger acute downstream regulation of assembled TJs. To address this problem, we developed a model of inducible tMLCK expression in fully differentiated epithelial monolayers, thereby overcoming limitations of previous studies (Gandhi et al., 1997; Hecht et al., 1996). Our data show that induction of tMLCK expression in mature monolayers causes MLC phosphorylation and is sufficient to cause increases in TJ permeability. These changes in TJ function are accompanied by morphological and biochemical TJ reorganization. Thus, these data are the first to show that MLC phosphorylation, in the absence of other more proximal signals, is sufficient to trigger the rapid regulation of assembled TJs.

Physiological TJ regulation is associated with size-selective increases in paracellular permeability (Fihn et al., 2000; Turner et al., 1997). We found that tMLCK-mediated MLC phosphorylation caused similar size-selective regulation of paracellular permeability. This increase in permeability requires tMLCK enzymatic activity, because MLCK inhibition reversed the effects of tMLCK expression. Moreover, the magnitude of MLC phosphorylation increases and TER decreases and the size selectivity of these changes induced by tMLCK expression were comparable to those following Na^+-nutrient co-transport (Table 1) (Atisook et al., 1990; Berglund et al., 2001; Fihn et al., 2000; Madara and Pappenheimer, 1987; Turner et al., 1997). Thus, TJ barrier regulation induced by MLC phosphorylation alone is similar to that induced following Na^+-nutrient co-transport.

Claudin protein expression determines TJ ion-permeability characteristics, but has not been shown to affect size selectivity (Furuse et al., 2001; Van Itallie et al., 2001). Moreover, changes in the pattern of claudin isoform expression have been reported in chronic disease (Heller et al., 2005; Prasad et al., 2005). The size-selective increases in TJ permeability to small hydrophilic solutes induced by tMLCK expression as well as the rapid onset and reversibility of these changes suggest that this mechanism of TJ regulation does not involve changes in claudin isoform expression. This is consistent with absence of apparent changes in synthesis or degradation of TJ proteins after tMLCK expression, as no change in expression of claudin-1, claudin-2, ZO-1 or occludin was detected. Thus, rather than the quantitatively large, ion-selective and long-lasting changes in permeability characteristics induced by changes in claudin isoform expression, MLC phosphorylation appears to represent a quantitatively small, size-selective and rapidly reversible form of TJ regulation. From a physiological perspective, this is an ideal mechanism to fine-tune TJ permeability in response to nutrient co-transport or pathogen exposure.

Our ultrastructural analysis of TJ architecture failed to reveal significant changes in strand organization that correlated with tMLCK-induced TJ regulation. Together with the absence of changes in claudin expression or distribution, this is consistent with the observation that claudin proteins are primary constituents of TJ strands (Furuse et al., 1998b). However, the distributions of two TJ proteins, ZO-1 and occludin, that interact directly with F-actin (Fanning et al., 1998; Wittchen et al., 1999) and with each other (Furuse et al., 1994) are

markedly altered by tMLCK-mediated MLC phosphorylation. The appearance of these proteins at the TJ assumes an undulating profile after tMLCK expression that can be reversed by MLCK inhibition. Moreover, the density of occludin-containing, detergent-insoluble membranes, but not membranes containing claudin-1 and claudin-2, was significantly increased by tMLCK expression, suggesting a change in the protein:lipid ratio of these fractions. The discordance between the observed occludin and ZO-1 redistribution and the lack of such changes in claudin-1 and claudin-2 distribution after tMLCK expression was not expected, particularly in light of the effect on barrier function. Several potential explanations for this difference can be considered. First, it is notable that ZO-1 and occludin, but not claudins, can interact directly with F-actin. Thus, it could be that this direct binding to actomyosin filaments is necessary for the observed TJ protein reorganization. Alternatively, homotypic interactions between claudin molecules on adjacent cells may serve to neutralize opposing actomyosin tension in adjacent cells: thereby preventing claudin proteins from being redistributed into undulated profiles. Biochemical analysis of TJ protein interactions in live epithelial cells within intact monolayers will be necessary to resolve these and other potential mechanisms. Nonetheless, it is clear from both morphological and biochemical data that tMLCK expression causes focal TJ reorganization.

Size-selective increases in paracellular permeability have been suggested to reflect an increase in the number of small pores within the TJ (Fihn et al., 2000). However, the structural correlate to this increase in pore number has not been defined. Some have speculated that the intrajunctional dilatations that appear following Na^+-nutrient co-transport are the site of these pores (Atisook and Madara, 1991). However, although tMLCK-mediated MLC phosphorylation did cause functional changes similar to those induced by Na^+-glucose co-transport, it did not induce the appearance of intrajunctional dilatations. Thus, these dilatations are not required for size-selective increases in TJ permeability and may not be related to MLC phosphorylation. This is consistent with our unpublished observations that MLCK inhibition, which prevents increased paracellular permeability following activation of Na^+-glucose co-transport in isolated intestinal mucosae (Turner et al., 1997), does not prevent formation of intrajunctional dilatations (J.R.T. and J. L. Madara, unpublished observations). It may therefore be that intrajunctional dilatations form in response to the osmotic gradient and water flux that follow transepithelial Na^+-glucose co-transport. Alternatively, the intrajunctional dilatations may require activation of one of the other signaling pathways triggered by Na^+-glucose co-transport (Shiue et al., 2005; Turner, 2000; Turner and Black, 2001; Turner et al., 2000; Zhao et al., 2004). Nevertheless, the structural correlate of the increases in permeability, i.e. the small size-selective pores induced by MLC phosphorylation, remains unknown. Although our data do not reveal the identity of these pores or their mechanism of assembly, it is tempting to speculate that the local disruptions in TJ architecture represented by ZO-1 and occludin undulations may be the sites of these pores.

In summary, the results of these studies show that tMLCK-mediated MLC phosphorylation is sufficient to trigger regulation of TJ barrier function in fully differentiated epithelial monolayers. This regulation is associated with biochemical and morphological reorganization of TJ proteins. Based on these results, we conclude that such reorganization secondary to MLC phosphorylation explains the reversible changes in TJ function. This general mechanism of TJ reorganization may underlie the acute TJ regulation seen in vitro and in vivo.

Materials and Methods

Generation of cell lines and preparation of monolayer cultures

The Tet-off inducible expression system (Gossen and Bujard, 1992) was established in stably transfected Caco-2BBe cell clones (Peterson and Mooseker, 1992; Yu et al., 2001). These cell lines were then stably cotransfected with a vector derived from pBI-L (Clontech, Palo Alto, CA) that expresses luciferase and truncated myosin light chain kinase (tMLCK) from a single Tet-transactivator transcriptional unit (Baron et al., 1995) and pTK hygromycin (Clontech) and selected using hygromycin.

Cells were grown as confluent monolayers on Transwell supports (Corning, Acton, MA), as described previously (Turner et al., 1997). Transwells inserts were maintained in media supplemented with 5 ng/ml of doxycycline, to prevent tMLCK expression during maturation, and studied 14-21 days post confluence. Induction of tMLCK was accomplished by culture in media without doxycycline. Complete suppression of tMLCK expression was ensured during terminal experiments with 25 ng/ml doxycycline.

mRNA analysis

Monolayers were scraped into Trizol (Invitrogen, Carlsbad, CA) and total RNA was purified, treated with DNase I (Invitrogen), and first strand cDNA synthesis carried out using Superscript II RT (Invitrogen) and oligo $(dT)_{12\text{-}18}$ primers. PCR amplification of tMLCK transcripts was for 30 cycles (forward primer: 5′-AAG-AAAGACTGGGATCGGGGAA-3′; reverse primer: 5′-CCGAAAGAGGGAAGT-ACC-3′). The identity of the 584 base pair PCR product was confirmed by restriction digestion with *Nsi*I, which generated fragments of 300 and 284 base pairs.

Analysis of MLCK activity and intracellular MLC phosphorylation

Confluent monolayers were washed and scraped into lysis buffer (20 mM MOPS pH 7.4, 2 mM $MgCl_2$, 0.2 mM $CaCl_2$, 1 mM DTT, 0.5% NP-40, 0.5% Triton X-100, 0.5 mM AEBSF, 0.4 mM aprotinin, 25 μM bestatin, 7.5 μM E-64, 10 μM leupeptin, 5 μM pepstatin, 2 mM imidazole, 1 mM sodium fluoride, 1.15 mM sodium molybdate, 1 mM sodium orthovanadate and 4 mM sodium tartrate). Total protein was measured (BCA assay, Pierce, Rockford, IL) and 0.15 μg lysate was incubated in a final reaction mixture with 10 μM recombinant purified intestinal epithelial MLC, 0.5 mM [γ-^{32}P]ATP, in 20 mM MOPS pH 7.4, 0.2 μM calmodulin, 0.2 mM $CaCl_2$ and 2 mM $MgCl_2$ at 30°C (Zolotarevsky et al., 2002). Parallel assays were also performed with 0.5 mM EDTA in place of calmodulin and divalent cations. After 30 minutes, reactions were stopped by addition of SDS-PAGE sample buffer and boiled. After SDS-PAGE, autoradiographs were scanned and analyzed using Sigma gel software (SPSS, Chicago, IL).

For analysis of intracellular (endogenous) MLC phosphorylation confluent monolayers were grown on 4.5 cm^2 Transwell inserts (Corning). Monolayers were scraped into lysis buffer (10 mM Tris pH 7.5, 50 mM NaCl, 0.5% Triton X-100, 0.1% SDS, 0.1% sodium deoxycholate, 0.5 mM AEBSF, 0.4 mM aprotinin, 25 μM bestatin, 7.5 μM E-64, 10 μM leupeptin and 5 μM pepstatin) and boiled. Samples were diluted with 3× SDS-PAGE sample buffer and analyzed by SDS-PAGE and immunoblot using antisera specific for Ser19 monophosphorylated MLC (Berglund et al., 2001). Chemiluminescent images were collected and analyzed using a Fluor-S-Max MultiImager system (Bio-Rad, Hercules, CA).

Quantitative analysis of phalloidin binding

Quantitative analysis of phalloidin binding was used to determine F-actin content based on the method of Howard and Oresajo (Howard and Oresajo, 1985a; Howard and Oresajo, 1985b). Cells were grown to confluence in media supplemented with 5ng/ml doxycycline and then transferred to media with or without 25 ng/ml doxycycline. Monolayers were fixed with 3% paraformaldehyde in HBSS at indicated times after tMLCK induction. After fixation the cell monolayers were washed twice with HBSS, permeabilized for 15 minutes in HBSS with 0.5% saponin (w/v), and incubated with 0.5 mM Alexa Fluor 488-conjugated phalloidin (Invitrogen) for 1 hour at room temperature. Unbound phalloidin was removed by five washes in HBSS. Bound Alexa Fluor 488-conjugated phalloidin was then extracted quantitatively by incubation for 18 hours at 4°C (in the dark) in 100% methanol. The fluorescent intensity of the extracted Alexa Fluor 488-conjugated phalloidin was measured on an Ultrospec 3300 fluorescent plate reader (Molecular

Dynamics, Sunnyvale, CA). All data were then normalized to the F-actin content of control monolayers incubated in medium with 25 ng/ml doxycycline.

Measurement of TER and paracellular permeability

TER of monolayers grown on 0.33 cm^2 Transwell supports was measured using agar bridges and Ag-AgCl calomel electrodes, as described previously (Turner et al., 1997). Paracellular permeability was assessed in monolayers grown on collagen-coated Snapwells (Corning) mounted in HBSS and placed in modified Üssing chambers (Physiologic Instruments, San Diego, CA), as described previously (Zolotarevsky et al., 2002).

Fluorescence microscopy

Monolayers were fixed in 1% paraformaldehyde in PBS and stained as described previously (Zolotarevsky et al., 2002). Rabbit polyclonal antibodies against ZO-1, occludin, claudin-1, claudin-2 and monoclonal anti-occludin were from Zymed (South San Francisco, CA). Alexa Fluor 488- and Alexa Fluor 594-conjugated goat anti-rabbit and goat anti-mouse antibodies, Alexa Fluor 488-conjugated phalloidin and Hoechst 33342 were from Invitrogen. Stained monolayers were mounted in Slowfade (Invitrogen) and images collected using 63× N.A. 1.32 or 100× N.A. 1.35 PLAN APO objectives mounted on a Leica DMLB microscope equipped with an 88000 filter set (Chroma Technology, Brattleboro, VT), motorized excitation wheels and *z*-motor (Ludl Electronic Products, Hawthorne, NY), and Roper Coolsnap HQ camera controlled by Metamorph 6 (Universal Imaging Corporation, Downingtown PA). *Z* stacks were collected at 0.2 μm intervals.

Image processing and analysis

Images were processed post-acquisition using Autodeblur 9 (AutoQuant Imaging, Watervliet, NY). Widefield fluorescence, adaptive blind, three-dimensional deconvolution was performed for ten iterations using low noise settings and an iteratively reconstructed point spread function. Each channel was deconvolved independently. Direct examination verified that the deconvolution process did not create new morphological features; as the images were similar, but with less out-of-plane haze, to those viewed directly through the widefield oculars. Moreover, images with essentially identical morphological features were obtained by confocal imaging using a Leica SP2 AOBS system over a range of pinhole settings. For presentation of 3D projections, deconvolved stacks were imported into AutoVisualize 9 (AutoQuant Imaging) and 3D hardware-generated maximum volume projections were created using matched settings for corresponding images. For *x-y* plane images, single deconvolved planes at the level of the TJ were selected based on the peak of ZO-1 labeling. The peak of occludin labeling was used to define the *z* plane of the TJ when ZO-1 was not labeled.

To quantify TJ profile undulations, well-orientated deconvolved *z* stacks were used. For semi-quantitative subjective analysis, the TJ profile between two adjacent tricellular zones was categorized as straight or undulated using coded images by a blinded observer. Six randomly chosen fields were counted for each condition. All TJ segments in each field counted were examined and the percentage of with undulations calculated.

For quantitative analysis we reasoned that undulations should increase junction length in en face profiles. To measure length, images were skeletonized using Metamorph 6 (supplementary material Fig. S1A,B) and actual linear junction length between two adjacent tricellular zones was determined using the fiber length measuring tool (supplementary material Fig. S1C). A straight line connecting the two tricellular zones was then drawn and hinged at up to two sites to maximize alignment over the junction (supplementary material Fig. S1D). The length of the hinged line was also measured. The actual linear junction length was normalized to the length of the hinged line for each TJ segment. The tight junction profile length is defined as the ratio between actual linear junction length and corresponding hinged line length. Measurements were performed on randomly chosen fields by a blinded observer. Forty segments were measured for each condition examined.

Freeze-fracture electron microscopy

Confluent monolayers grown on 44 cm^2 Transwell supports were induced as described above and fixed in 2% glutaraldehyde in PBS for 20 minutes at 4°C. After rinsing in PBS, monolayers were scraped from the filter and infiltrated with 25% glycerol in 0.1 M cacodylate pH 7.3 for 60 minutes at 4°C. Cell pellets were frozen in liquid nitrogen slush and then freeze fractured at –115°C in a Balzers 400 freeze-fracture unit (Balzers, Liechtenstein). After cleaning with sodium hypochlorite, replicas were examined using a Philips 301 electron microscope. TJ height and number of parallel strands within the TJs was counted at 1 cm intervals on coded electron micrographs at a magnification of 62,500× (Lynch et al., 1993).

Isolation and analysis of detergent-insoluble membrane fractions

Detergent-insoluble membrane fractions were prepared by scraping monolayers grown on 44 cm^2 Transwell inserts into 4°C lysis buffer (150 mM NaCl, 20 mM Tris-HCl pH 7.4, 1% Triton X-100, containing 0.5 mM AEBSF, 0.4 mM aprotinin, 25 μM bestatin, 7.5 μM E-64, 10 μM leupeptin, 5 μM pepstatin, 2 mM imidazole, 1 mM sodium fluoride, 1.15 mM sodium molybdate, 1 mM sodium orthovanadate and 4 mM sodium tartrate). Nuclei and cellular debris were removed by a low speed centrifugation (1000 ***g*** for 10 minutes). The supernatant was diluted with an equal volume of 80% sucrose, layered beneath a preformed 4-30% sucrose (w/v) gradient, and centrifuged at 39,000 ***g*** for 18 hours. Fractions (0.5 ml) were collected from the top of the gradient and the sucrose concentration in each fraction was measured by refractometry. Equal volumes of the fractions were combined 1:1 with 2× Laemmli SDS-PAGE sample buffer, separated by 4-20% gradient SDS-PAGE and transferred to PVDF membranes for immunoblotting. Primary antibodies were incubated overnight in blocking buffer. Rabbit polyclonal antibodies against actin, occludin, claudin-1 and claudin-2 were used at 0.5 μg/ml (Zymed). GM1 ganglioside was detected with peroxidase-conjugated cholera toxin B subunit (0.5 nM, Sigma). Membranes were developed using chemiluminsecent detection reagents (Pierce) and images were collected and analyzed using a Fluor-S-Max MultiImager (Bio-Rad).

Statistical analysis

Data are presented as mean ± s.e.m. All experiments were performed with triplicate or greater samples, and data shown are representative of three or more independent studies. *P* values were determined by two-tailed Student's *t*-test and were considered to be significant if $P<0.05$.

We are pleased to acknowledge the expert technical assistance of Sara Palkon and Yingmin Wang. This work was supported by the National Institutes of Health (DK61931 and DK68271 to J.R.T., DK53056, DK48106, and DK57827 to W.I.L., and HL25822 and HL36781 to E.E.S.), the Crohn's Colitis Foundation of America (to J.R.T.), the University of Chicago Digestive Disease Center (DK42086), and the University of Chicago Cancer Center (CA14599).

References

Amasheh, S., Meiri, N., Gitter, A. H., Schoneberg, T., Mankertz, J., Schulzke, J. D. and Fromm, M. (2002). Claudin-2 expression induces cation-selective channels in tight junctions of epithelial cells. *J. Cell Sci.* **115**, 4969-4976.

Atisook, K. and Madara, J. L. (1991). An oligopeptide permeates intestinal tight junctions at glucose-elicited dilatations. Implications for oligopeptide absorption. *Gastroenterology* **100**, 719-724.

Atisook, K., Carlson, S. and Madara, J. L. (1990). Effects of phlorizin and sodium on glucose-elicited alterations of cell junctions in intestinal epithelia. *Am. J. Physiol.* **258**, C77-C85.

Balda, M. S., Whitney, J. A., Flores, C., Gonzalez, S., Cereijido, M. and Matter, K. (1996). Functional dissociation of paracellular permeability and transepithelial electrical resistance and disruption of the apical- basolateral intramembrane diffusion barrier by expression of a mutant tight junction membrane protein. *J. Cell Biol.* **134**, 1031-1049.

Baron, U., Freundlieb, S., Gossen, M. and Bujard, H. (1995). Co-regulation of two gene activities by tetracycline via a bidirectional promoter. *Nucleic Acids Res.* **23**, 3605-3606.

Benais-Pont, G., Punn, A., Flores-Maldonado, C., Eckert, J., Raposo, G., Fleming, T. P., Cereijido, M., Balda, M. S. and Matter, K. (2003). Identification of a tight junction-associated guanine nucleotide exchange factor that activates Rho and regulates paracellular permeability. *J. Cell Biol.* **160**, 729-740.

Berglund, J. J., Riegler, M., Zolotarevsky, Y., Wenzl, E. and Turner, J. R. (2001). Regulation of human jejunal transmucosal resistance and MLC phosphorylation by Na^+-glucose cotransport. *Am. J. Physiol. Gastrointest. Liver Physiol.* **281**, G1487-G1493.

Bruewer, M., Luegering, A., Kucharzik, T., Parkos, C. A., Madara, J. L., Hopkins, A. M. and Nusrat, A. (2003). Proinflammatory cytokines disrupt epithelial barrier function by apoptosis-independent mechanisms. *J. Immunol.* **171**, 6164-6172.

Bruewer, M., Utech, M., Ivanov, A. I., Hopkins, A. M., Parkos, C. A. and Nusrat, A. (2005). Interferon-gamma induces internalization of epithelial tight junction proteins via a macropinocytosis-like process. *FASEB J.* **19**, 923-933.

Clayburgh, D. R., Rosen, S., Witkowski, E. D., Wang, F., Blair, S., Dudek, S., Garcia, J. G., Alverdy, J. C. and Turner, J. R. (2004). A differentiation-dependent splice variant of myosin light chain kinase, MLCK1, regulates epithelial tight junction permeability. *J. Biol. Chem.* **279**, 55506-55513.

Clayburgh, D. R., Barrett, T. A., Tang, Y., Meddings, J. B., Van Eldik, L. J., Watterson, D. M., Clarke, L. L., Mrsny, R. J. and Turner, J. R. (2005). Epithelial myosin light chain kinase-dependent barrier dysfunction mediates T cell activation-induced diarrhea in vivo. *J. Clin. Invest.* **115**, 2702-2715.

Dahan, S., Dalmasso, G., Imbert, V., Peyron, J. F., Rampal, P. and Czerucka, D. (2003). Saccharomyces boulardii interferes with enterohemorrhagic Escherichia coli-induced signaling pathways in T84 cells. *Infect. Immun.* **71**, 766-773.

Edens, H. A., Levi, B. P., Jaye, D. L., Walsh, S., Reaves, T. A., Turner, J. R., Nusrat, A. and Parkos, C. A. (2002). Neutrophil transepithelial migration: evidence for sequential, contact-dependent signaling events and enhanced paracellular permeability independent of transjunctional migration. *J. Immunol.* **169**, 476-486.

Fanning, A. S., Jameson, B. J., Jesaitis, L. A. and Anderson, J. M. (1998). The tight junction protein ZO-1 establishes a link between the transmembrane protein occludin and the actin cytoskeleton. *J. Biol. Chem.* **273**, 29745-29753.

Fihn, B. M., Sjoqvist, A. and Jodal, M. (2000). Permeability of the rat small intestinal epithelium along the villus-crypt axis: effects of glucose transport. *Gastroenterology* **119**, 1029-1036.

Francis, S. A., Kelly, J. M., McCormack, J., Rogers, R. A., Lai, J., Schneeberger, E. E. and Lynch, R. D. (1999). Rapid reduction of MDCK cell cholesterol by methyl-beta-cyclodextrin alters steady state transepithelial electrical resistance. *Eur. J. Cell Biol.* **78**, 473-484.

Furuse, M., Itoh, M., Hirase, T., Nagafuchi, A., Yonemura, S. and Tsukita, S. (1994). Direct association of occludin with ZO-1 and its possible involvement in the localization of occludin at tight junctions. *J. Cell Biol.* **127**, 1617-1626.

Furuse, M., Fujita, K., Hiiragi, T., Fujimoto, K. and Tsukita, S. (1998a). Claudin-1 and -2: novel integral membrane proteins localizing at tight junctions with no sequence similarity to occludin. *J. Cell Biol.* **141**, 1539-1550.

Furuse, M., Sasaki, H., Fujimoto, K. and Tsukita, S. (1998b). A single gene product, claudin-1 or -2, reconstitutes tight junction strands and recruits occludin in fibroblasts. *J. Cell Biol.* **143**, 391-401.

Furuse, M., Furuse, K., Sasaki, H. and Tsukita, S. (2001). Conversion of zonulae occludentes from tight to leaky strand type by introducing claudin-2 into Madin-Darby canine kidney I cells. *J. Cell Biol.* **153**, 263-272.

Gandhi, S., Lorimer, D. D. and de Lanerolle, P. (1997). Expression of a mutant myosin light chain that cannot be phosphorylated increases paracellular permeability. *Am. J. Physiol.* **272**, F214-F221.

Goeckeler, Z. M. and Wysolmerski, R. B. (1995). Myosin light chain kinase-regulated endothelial cell contraction: the relationship between isometric tension, actin polymerization, and myosin phosphorylation. *J. Cell Biol.* **130**, 613-627.

Gopalakrishnan, S., Raman, N., Atkinson, S. J. and Marrs, J. A. (1998). Rho GTPase signaling regulates tight junction assembly and protects tight junctions during ATP depletion. *Am. J. Physiol.* **275**, C798-C809.

Gossen, M. and Bujard, H. (1992). Tight control of gene expression in mammalian cells by tetracycline-responsive promoters. *Proc. Natl. Acad. Sci. USA* **89**, 5547-5551.

Guerriero, V., Jr, Russo, M. A., Olson, N. J., Putkey, J. A. and Means, A. R. (1986). Domain organization of chicken gizzard myosin light chain kinase deduced from a cloned cDNA. *Biochemistry* **25**, 8372-8381.

Hecht, G., Pestic, L., Nikcevic, G., Koutsouris, A., Tripuraneni, J., Lorimer, D. D., Nowak, G., Guerriero, V., Jr, Elson, E. L. and Lanerolle, P. D. (1996). Expression of the catalytic domain of myosin light chain kinase increases paracellular permeability. *Am. J. Physiol.* **271**, C1678-C1684.

Heller, F., Florian, P., Bojarski, C., Richter, J., Christ, M., Hillenbrand, B., Mankertz, J., Gitter, A. H., Burgel, N., Fromm, M. et al. (2005). Interleukin-13 is the key effector Th2 cytokine in ulcerative colitis that affects epithelial tight junctions, apoptosis, and cell restitution. *Gastroenterology* **129**, 550-564.

Hirase, T., Kawashima, S., Wong, E. Y., Ueyama, T., Rikitake, Y., Tsukita, S., Yokoyama, M. and Staddon, J. M. (2001). Regulation of tight junction permeability and occludin phosphorylation by RhoA-p160ROCK-dependent and -independent mechanisms. *J. Biol. Chem.* **276**, 10423-10431.

Hopkins, A. M., Walsh, S. V., Verkade, P., Boquet, P. and Nusrat, A. (2003). Constitutive activation of Rho proteins by CNF-1 influences tight junction structure and epithelial barrier function. *J. Cell Sci.* **116**, 725-742.

Howard, T. H. and Oresajo, C. O. (1985a). The kinetics of chemotactic peptide-induced change in F-actin content, F-actin distribution, and the shape of neutrophils. *J. Cell Biol.* **101**, 1078-1085.

Howard, T. H. and Oresajo, C. O. (1985b). A method for quantifying F-actin in chemotactic peptide activated neutrophils: study of the effect of tBOC peptide. *Cell Motil.* **5**, 545-557.

Ikebe, M., Hartshorne, D. J. and Elzinga, M. (1987). Phosphorylation of the 20,000-dalton light chain of smooth muscle myosin by the calcium-activated, phospholipid-dependent protein kinase. Phosphorylation sites and effects of phosphorylation. *J. Biol. Chem.* **262**, 9569-9573.

Ito, M., Guerriero, V., Jr, Chen, X. M. and Hartshorne, D. J. (1991). Definition of the inhibitory domain of smooth muscle myosin light chain kinase by site-directed mutagenesis. *Biochemistry* **30**, 3498-3503.

Ivanov, A. I., McCall, I. C., Parkos, C. A. and Nusrat, A. (2004a). Role for actin filament turnover and a myosin II motor in cytoskeleton-driven disassembly of the epithelial apical junctional complex. *Mol. Biol. Cell* **15**, 2639-2651.

Ivanov, A. I., Nusrat, A. and Parkos, C. A. (2004b). Endocytosis of epithelial apical junctional proteins by a clathrin-mediated pathway into a unique storage compartment. *Mol. Biol. Cell* **15**, 176-188.

Jou, T. S., Schneeberger, E. E. and James Nelson, W. (1998). Structural and functional regulation of tight junctions by rhoA and rac1 small GTPases. *J. Cell Biol.* **142**, 101-115.

Katoh, K., Kano, Y., Amano, M., Onishi, H., Kaibuchi, K. and Fujiwara, K. (2001). Rho-kinase-mediated contraction of isolated stress fibers. *J. Cell Biol.* **153**, 569-584.

Lukas, T. J., Mirzoeva, S., Slomczynska, U. and Watterson, D. M. (1999). Identification of novel classes of protein kinase inhibitors using combinatorial peptide chemistry based on functional genomics knowledge. *J. Med. Chem.* **42**, 910-919.

Lynch, R. D., Tkachuk, L. J., Ji, X., Rabito, C. A. and Schneeberger, E. E. (1993). Depleting cell cholesterol alters calcium-induced assembly of tight junctions by monolayers of MDCK cells. *Eur. J. Cell Biol.* **60**, 21-30.

Ma, T. Y., Nguyen, D., Bui, V., Nguyen, H. and Hoa, N. (1999). Ethanol modulation of intestinal epithelial tight junction barrier. *Am. J. Physiol.* **276**, G965-G974.

Ma, T. Y., Iwamoto, G. K., Hoa, N. T., Akotia, V., Pedram, A., Boivin, M. A. and Said, H. M. (2004). TNF-alpha-induced increase in intestinal epithelial tight junction permeability requires NF-kappa B activation. *Am. J. Physiol. Gastrointest. Liver Physiol.* **286**, G367-G376.

Ma, T. Y., Boivin, M. A., Ye, D., Pedram, A. and Said, H. M. (2005). Mechanism of TNF-{alpha} modulation of Caco-2 intestinal epithelial tight junction barrier: role of myosin light-chain kinase protein expression. *Am. J. Physiol. Gastrointest. Liver Physiol.* **288**, G422-G430.

Madara, J. L. and Pappenheimer, J. R. (1987). Structural basis for physiological regulation of paracellular pathways in intestinal epithelia. *J. Membr. Biol.* **100**, 149-164.

Madara, J. L., Carlson, S. and Anderson, J. M. (1993). ZO-1 maintains its spatial distribution but dissociates from junctional fibrils during tight junction regulation. *Am. J. Physiol.* **264**, C1096-C1101.

McCarthy, K. M., Skare, I. B., Stankewich, M. C., Furuse, M., Tsukita, S., Rogers, R. A., Lynch, R. D. and Schneeberger, E. E. (1996). Occludin is a functional component of the tight junction. *J. Cell Sci.* **109**, 2287-2298.

Nusrat, A., Giry, M., Turner, J. R., Colgan, S. P., Parkos, C. A., Carnes, D., Lemichez, E., Boquet, P. and Madara, J. L. (1995). Rho protein regulates tight junctions and perijunctional actin organization in polarized epithelia. *Proc. Natl. Acad. Sci. USA* **92**, 10629-10633.

Nusrat, A., Parkos, C. A., Verkade, P., Foley, C. S., Liang, T. W., Innis-Whitehouse, W., Eastburn, K. K. and Madara, J. L. (2000). Tight junctions are membrane microdomains. *J. Cell Sci.* **113**, 1771-1781.

Nusrat, A., von Eichel-Streiber, C., Turner, J. R., Verkade, P., Madara, J. L. and Parkos, C. A. (2001). Clostridium difficile toxins disrupt epithelial barrier function by altering membrane microdomain localization of tight junction proteins. *Infect. Immun.* **69**, 1329-1336.

Peterson, M. D. and Mooseker, M. S. (1992). Characterization of the enterocyte-like brush border cytoskeleton of the C2BBe clones of the human intestinal cell line, Caco-2. *J. Cell Sci.* **102**, 581-600.

Philpott, D. J., McKay, D. M., Mak, W., Perdue, M. H. and Sherman, P. M. (1998). Signal transduction pathways involved in enterohemorrhagic Escherichia coli-induced alterations in T84 epithelial permeability. *Infect. Immun.* **66**, 1680-1687.

Prasad, S., Mingrino, R., Kaukinen, K., Hayes, K. L., Powell, R. M., MacDonald, T. T. and Collins, J. E. (2005). Inflammatory processes have differential effects on Claudins 2, 3 and 4 in colonic epithelial cells. *Lab. Invest.* **85**, 1139-1162.

Savkovic, S. D., Koutsouris, A. and Hecht, G. (2003). PKC zeta participates in activation of inflammatory response induced by enteropathogenic E. coli. *Am. J. Physiol. Cell Physiol.* **285**, C512-C521.

Scott, K. G., Meddings, J. B., Kirk, D. R., Lees-Miller, S. P. and Buret, A. G. (2002). Intestinal infection with Giardia spp. reduces epithelial barrier function in a myosin light chain kinase-dependent fashion. *Gastroenterology* **123**, 1179-1190.

Shen, L. and Turner, J. R. (2005). Actin depolymerization disrupts tight junctions via caveolae-mediated endocytosis. *Mol. Biol. Cell* **16**, 3919-3936.

Shifflett, D. E., Clayburgh, D. R., Koutsouris, A., Turner, J. R. and Hecht, G. A. (2005). Enteropathogenic E. coli disrupts tight junction barrier function and structure in vivo. *Lab. Invest.* **85**, 1308-1324.

Shiue, H., Musch, M. W., Wang, Y., Chang, E. B. and Turner, J. R. (2005). Akt2 phosphorylates ezrin to trigger NHE3 translocation and activation. *J. Biol. Chem.* **280**, 1688-1695.

Simon, D. B., Lu, Y., Choate, K. A., Velazquez, H., Al-Sabban, E., Praga, M., Casari, G., Bettinelli, A., Colussi, G., Rodriguez-Soriano, J. et al. (1999). Paracellin-1, a renal tight junction protein required for paracellular Mg2+ resorption. *Science* **285**, 103-106.

Simonovic, I., Rosenberg, J., Koutsouris, A. and Hecht, G. (2000). Enteropathogenic Escherichia coli dephosphorylates and dissociates occludin from intestinal epithelial tight junctions. *Cell Microbiol.* **2**, 305-315.

Spitz, J., Yuhan, R., Koutsouris, A., Blatt, C., Alverdy, J. and Hecht, G. (1995). Enteropathogenic Escherichia coli adherence to intestinal epithelial monolayers diminishes barrier function. *Am. J. Physiol.* **268**, G374-G379.

Sugi, K., Musch, M. W., Field, M. and Chang, E. B. (2001). Inhibition of Na+,K+-ATPase by interferon gamma down-regulates intestinal epithelial transport and barrier function. *Gastroenterology* **120**, 1393-1403.

Tomson, F. L., Koutsouris, A., Viswanathan, V. K., Turner, J. R., Savkovic, S. D. and Hecht, G. (2004). Differing roles of protein kinase C-zeta in disruption of tight junction barrier by enteropathogenic and enterohemorrhagic Escherichia coli. *Gastroenterology* **127**, 859-869.

Turner, J. R. (2000). Show me the pathway! Regulation of paracellular permeability by Na^+-glucose cotransport. *Adv. Drug Deliv. Rev.* **41**, 265-281.

Turner, J. R. and Black, E. D. (2001). NHE3-dependent cytoplasmic alkalinization is triggered by Na^+-glucose cotransport in intestinal epithelia. *Am. J. Physiol. Cell Physiol.* **281**, C1533-C1541.

Turner, J. R., Rill, B. K., Carlson, S. L., Carnes, D., Kerner, R., Mrsny, R. J. and Madara, J. L. (1997). Physiological regulation of epithelial tight junctions is associated with myosin light-chain phosphorylation. *Am. J. Physiol.* **273**, C1378-C1385.

Turner, J. R., Black, E. D., Ward, J., Tse, C. M., Uchwat, F. A., Alli, H. A., Donowitz, M., Madara, J. L. and Angle, J. M. (2000). Transepithelial resistance can be regulated by the intestinal brush border Na^+-H^+ exchanger NHE3. *Am. J. Physiol. Cell Physiol.* **279**, C1918-C1924.

Van Itallie, C., Rahner, C. and Anderson, J. M. (2001). Regulated expression of claudin-4 decreases paracellular conductance through a selective decrease in sodium permeability. *J. Clin. Invest.* **107**, 1319-1327.

Walsh, S. V., Hopkins, A. M., Chen, J., Narumiya, S., Parkos, C. A. and Nusrat, A.

(2001). Rho kinase regulates tight junction function and is necessary for tight junction assembly in polarized intestinal epithelia. *Gastroenterology* **121**, 566-579.

Wang, F., Graham, W. V., Wang, Y., Witkowski, E. D., Schwarz, B. T. and Turner, J. R. (2005). Interferon-gamma and tumor necrosis factor-alpha synergize to induce intestinal epithelial barrier dysfunction by up-regulating myosin light chain kinase expression. *Am. J. Pathol.* **166**, 409-419.

Wittchen, E. S., Haskins, J. and Stevenson, B. R. (1999). Protein interactions at the tight junction. Actin has multiple binding partners, and ZO-1 forms independent complexes with ZO-2 and ZO-3. *J. Biol. Chem.* **274**, 35179-35185.

Wolf, A. A., Jobling, M. G., Wimer-Mackin, S., Ferguson-Maltzman, M., Madara, J. L., Holmes, R. K. and Lencer, W. I. (1998). Ganglioside structure dictates signal transduction by cholera toxin and association with caveolae-like membrane domains in polarized epithelia. *J. Cell Biol.* **141**, 917-927.

Yu, Y., Rishi, A. K., Turner, J. R., Liu, D., Black, E. D., Moshier, J. A. and Majumdar, A. P. (2001). Cloning of a novel EGFR-related peptide: a putative negative regulator of EGFR. *Am. J. Physiol. Cell Physiol.* **280**, C1083-C1089.

Yuhan, R., Koutsouris, A., Savkovic, S. D. and Hecht, G. (1997). Enteropathogenic Escherichia coli-induced myosin light chain phosphorylation alters intestinal epithelial permeability. *Gastroenterology* **113**, 1873-1882.

Zhao, H., Shiue, H., Palkon, S., Wang, Y., Cullinan, P., Burkhardt, J. K., Musch, M. W., Chang, E. B. and Turner, J. R. (2004). Ezrin regulates NHE3 translocation and activation after Na+-glucose cotransport. *Proc. Natl. Acad. Sci. USA* **101**, 9485-9490.

Zolotarevsky, Y., Hecht, G., Koutsouris, A., Gonzalez, D. E., Quan, C., Tom, J., Mrsny, R. J. and Turner, J. R. (2002). A membrane-permeant peptide that inhibits MLC kinase restores barrier function in in vitro models of intestinal disease. *Gastroenterology* **123**, 163-172.